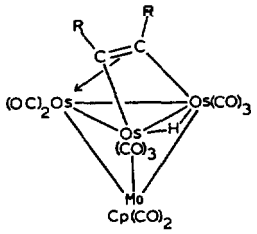

a

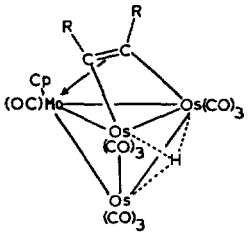

b

3a : R=Tol
4a : R=H
5a : R=CO_2Et

5b : R=CO_2Et

With the two alkynes [R=H or Tol (=*p*-C_6H_4Me)] only symmetrical isomers (**3a** and **4a**) are formed, while both symmetrical (**5a**) and unsymmetrical (**5b**) isomers are obtained with an electron-withdrawing alkyne (R=CO_2Et). The ^{1}H-NMR spectra of symmetrical isomers **3a**, **4a** and **5a** reveal that both substituents R_2 in an alkyne are equivalent. With the tungsten analogue of **5b**, two distinct ethyl groups of resonances were observed in the ^{1}H-NMR spectrum, indicating its unsymmetrical structure.[2] The unsymmetrical nature of this tungsten analogue is due to an unsymmetrical ligand arrangement with respect to the tungsten atom. The ^{1}H-NMR spectrum of **5b** at room temperature, however, exhibits a single resonance for the two ethyl groups. This may indicate that two ligands, a carbonyl and a cyclopentadienyl ligands, on the molybdenum atom undergo a fast two-fold exchange at room temperature. The close similarities of the carbonyl regions of the IR spectra between the tungsten[2] and molybdenum complexes indicate the structural correspondence in the various alkyne clusters.

The diaryl alkyne WOs_3 clusters were reported to undergo scission of the alkyne ligand to provide dialkylidyne compounds.[2] However, attempted alkyne scission reaction with compounds **3a**, 4a and **5a** did not produce any alkyne scission products and only resulted in extensive decomposition of the starting materials. The symmetrical isomer **5a** isomerizes to the unsymmetrical isomer **5b** upon heating. Kinetic measurements for the isomerization **5a**→**5b** were carried out at 80℃ by ^{1}H-NMR spectroscopy. Crystals of **5a** were dissolved in toluene-d_8 in an NMR tube, and signals due to **5b** were observed to grow in as a function of time. Relative concentrations of the two isomers were measured by integration of the peaks at δ −21.29 due to μ-H of **5a** and at δ −21.57 due to μ_3-H of **5b** in the ^{1}H-NMR spectrum as is shown in Figure 1. The two isomers are in equilibrium, and analysis according to reversible first order kinetics gives good fits of experimental data: $K_{eq}=[\mathbf{5a}]/[\mathbf{5b}]=0.749\pm0.004$, $k_{obs}=(4.22\pm0.23)\times10^{-4}$ s^{-1}, $k_1=(1.81\pm10)\times10^{-4}$ s^{-1}, and $k_{-1}=(2.41\pm0.13)\times10^{-4}$ s^{-1} (see Figure 2). These data compare with $k=(4.1\pm0.2)\times10^{-5}$ s^{-1} at 100℃ reported in the irreversible isomerization of $CpWOs_3(CO)_{10}[\mu_3\text{-}\eta^2\text{-}C_2(CO_2Et)_2](\mu\text{-H})$.[2]

Acknowledgement. We are grateful to the Korea Science and Engineering Foundation for financial support of this work.

References

1. (a) N. T. Allison, J. R. Fritch, K. P. C. Vollhardt, and E. C. Walborsky, *J. Am. Chem. Soc.*, **105**, 1384 (1983); (b) A. D. Clauss, J. R. Shapley, C. N. Wilker, and R. Hoffmann, *Organometallics*, 3, 619 (1984); (c) E. Sappa, A. Tiripicchio, A. J. Carty, and G. E. Toogood, *Prog. Inorg. Chem.*, **35**, 437 (1987).
2. (a) J. T. Park, J. R. Shapley, M. R. Churchill, and C. Bueno, *J. Am. Chem. Soc.*, **105**, 6182 (1983); (b) J. T. Park, J. R. Shapley, C. Bueno, J. W. Ziller, and M. R. Churchill, *Organometallics*, 7, 2307 (1988).
3. (a) B. F. G. Johnson, J. Lewis, and D. A. Pippard, *J. Chem. Soc., Dalton Trans.*, 407 (1981); (b) J. T. Park and J. R. Shapley, *Bull. Korean Chem. Soc.*, **11**, 531 (1990).
4. E. O. Fischer, *Inorg. Synth.*, 7, 136 (1963).
5. M. R. Churchill, F. J. Hollander, J. R. Shapley, and D. S. Foose, *J. Chem. Soc., Chem. Comm.*, 534 (1978).
6. L.-Y. Hsu, W.-L. Hsu, D.-Y. Jan, and S. G. Shroe, *Organometallics*, 5, 1041 (1986).

The Surface Composition of Cu-Mn Alloys in Ultrahigh Vacuum and in the Presence of Oxygen

Cheonho Yoon*

Department of Chemistry, Myongji University, Yongin, Kyonggi-do 449-728

Received July 11, 1992

In relation to the materials design, plenty of chemical and physical properties of alloys depend makedly on natures of surfaces and interfaces. Nowadays it is necessary to understand the relationship between externally controllable factors such as the bulk composition, temperature and ambient condition, and surface properties such as the surface compositon, surface structure and chemical activity. In particular, the information about the surface composition of alloys is of great importance. Generally surface composition of the alloys greatly differ from bulk, so called surface segregation. Reactions involved in the catalysis, oxidation, corrosion, *etc.* are known to be sensitive to surface composition.[1-3] Therefore characterization of alloy surfaces with respect to composition and reactivity is essential for understanding surface chemistry and for controlling materials performance.

In this note, first, surface composition is predicted based on unified model. Second, surface composition of four Cu-Mn alloys has been followed by means of X-ray photoelectron spectroscopy (XPS), one of the well established surface characterization techniques, as a function of annealing in ultra high vacuum and oxygen chemisorption.

Model Prediction of Surface Compositon of Cu-Mn Alloys

If there is no phase separation and no ordered phase in

Table 1. Thermodynamic Properties of Cu, Mn, and Cu-Mn Alloys[8-11]

Thermodynamic properties	Cu	Mn	Cu-Mn Alloys
Crystal structure	fcc	fcc	
Surface energy (mJ/m²)			
Experimental (averaged)	1327	1100	
Miedema model	1850	1600	
Heat of sublimation (kJ/g-at)	336.8	283.3	
Melting point (℃) (averaged)	1083	1244	
Molar volume (cm³/mole)			
Miedema model	3.7	3.8	
Bulk modulus (kg/cm²×10⁶)	1.355	0.6083	
Shear modulus (kg/cm²×10⁶)	0.46	0.78	
Atomic radius (Å)	1.28	1.12	
Bond strength (kJ/mol)	343	402	
Heat of solution (kJ/mole)			
Miedema			14

the bulk of a binary alloy, *A-B* (solute *A* and sevent *B*), surface concentration can be related to bulk concentration through the following equation, assuming negligible change in entropy.[1,4,5]

$$\frac{X_A^s}{X_B^s}=\frac{X_A^b}{X_B^b}\exp\left(-\frac{\Delta H_{segr}}{RT}\right) \quad (1)$$

where X_A^b and X_B^b are the concentrations of *A* and *B* in the bulk, X_A^s and X_B^s those on the surface, and ΔH_{segr} the heat of segregation or the enthalpy change when one gram-atom of *A* in the bulk is moved to the surface.

For the first time, the unified model is proposed and utilized to estimate the heat of segregation.

$$\Delta H_{segr}=\frac{f}{3}\left[\frac{g}{f}(\gamma_A-\gamma_B)\,V_A^{2/3}-H_{sol}(A,B)\right] - \frac{6KG\,r_A r_B(r_A-r_B)^2}{3K r_A+4G r_B}+(Z_A E_{AC}\,\theta_A-Z_B E_{BC}\,\theta_B) \quad (2)$$

The model consists of four contributions related to the surface energy (γ), heat of solution (H_{sol}), atomic size (r), and chemisorption energy (E). Further details of the terminology in Eq. (2) can be found in the references.[5-7]

Surface composition profile of Cu-Mn alloys can be semi-quantitatively predicted from available thermodynamic values. Thermodynamic properties of copper, manganese and Cu-Mn alloys are given in Table 1. Of course, wide variance in the thermodynamic quantities from the literature requires critical selection and estimation.[8-11] Based on the unified model, the heats of segregation were estimated. Calculated surface composition is plotted as a function of bulk composition for Cu-Mn alloys at 500℃, along with experimetal data, in Figure 1. Figure 1a predicts the first layer composition of manganese as a function of bulk composition for the clean surfaces. The enhanced enrichment in manganese of the surface layer when 0.1 monolayer oxygen is covered on the surface is shown in Figure 1b.

For the clean surfaces, the estimated ΔH_{segr}, −18.6 kJ/mole, is well compared with −17 kJ/mole calculated from the empirical relation given by Seah.[3] The surface enrichment of manganese for the clean Cu-Mn alloys is associated mainly with difference is the surface energies of copper and manganese (−12.7 kJ/mole). Contributions of the heat of solution of Cu-Mn alloys and difference in the atomic sizes of copper and manganese to the heat of segregation of Cu-Mn alloys (−3.4 and −2.6 kJ/mole, respectively) are not very critical. However, a contribution of oxygen interaction with the alloy surfaces to the heat of segregation (*e.g.*, −6.0 and −11.9 kJ/mole for 0.1 and 0.2 monolayer oxygen coverage, respectively) is quite crucial, depending on oxygen coverage, and is a main driving force of the manganese segregation in the presence of oxygen.

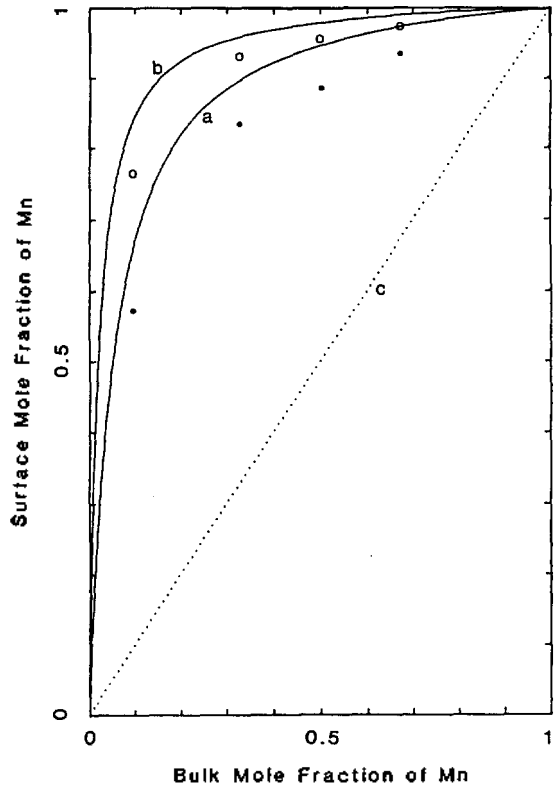

Figure 1. Surface composition of Cu-Mn alloys using the unified Miedema model at 500℃: (a) in vacuum (theoretical), (b) with 0.1 monolayer oxygen coverage (theoretical), (c) on segregation, (●) in vacuum (experimental), (○) with 0.1 monolayer oxygen coverage (experimental).

XPS Measurements of the Surface Composition of Cu-Mn Alloys

Cu-Mn alloys were prepared by an arc meltig device from copper shot (99.9999%, Johnson Matthey) and manganese flake (99.995%, Johnson Matthey). The alloys were abraded with sandpaper (600 grit alumina) and polished successively with 30, 15, 6 and 1 μm diamond paste. The alloys were found to be homogeneous after several remelting and turning cycles. The alloy samples examined were Cu-Mn (10%), Cu-Mn (33%), Cu-Mn (50%), and Cu-Mn (67%). Research-grade oxygen (Ashland Chemical) and sputter-grade argon (99.9999%, Scott Environment Technology) were used and manipulated in an ancillary chamber attached to the analytical chamber. Each alloy surface was cleaned by sputter bombardment with

argon ions at the pressure of 5×10^{-6} Torr and ion energy of 2500 eV for 30 min. Subsequently the alloy was subject to annealing at 500℃ in ultrahigh vacuum for 1 h, and then its XPS spectra were obtained. After admission of 0.1 monolayer oxygen, immediately specta were taken to study initial adsorption phenomena. XPS spectra were taken with an electron spectrometer (PHI Model 548) equipped with a data processing system. The spectral areas determined by computer integration were corrected for instrumental parameters, photoionization cross-section, and difference in electron mean-free-paths. The results were quantitatively interpreted with a novel calibration method.[12,13] The experimental data in Figure 1 indicate that the surface becomes enriched with maganeses by annealing in vacuum and that the adsorption of oxygen on the annealed surface causes enrichment. This is in qualitative agreement with those of the model predictions. Upon adsorbing oxygen, the observed manganese segregation seems to be induced not by the initial stage of oxidation (or the surface oxide formation), but mainly by the oxygen chemisoption. It is supported by the fact that any surface oxides were not observed at 530 eV right after the adsorption of oxygne on the annealed surface. For the clean surfaces, the heat of segregation of -15.2 ± 1.4 kJ/mole was obtained from the slope of Arrhenius plot of XPS data and is closed to the estimated value.

Cu-Mn alloys have attracted great scientific and technological interest due to their strong activity in CO oxidation, unusually high mechanical damping characteristic, and reversible shape memory effect. Nevertheless, surface segregation for Cu-Mn alloys has never bee studied with the exception of Hedge *et al.*[14] They obtained the heat of segregation of -25 kJ/mole for Cu-Mn (5%) alloy from Arrhenius plots of the Auger and XPS data. It appears to be exaggerated compared with the model estimation and XPS measurements here, probably due to the surface oxide formation. Since the initial monoxide formation begins even at 2 L exposure, special attention should be paid to designing experimentation.

The unified model presented here provides a meaningful semiquantitative framework for describing the surface segregation of alloys, as demonstrated by XPS measurements, and could be generalized and extended to other alloy systems. It is useful for estimating the surface compositionn versus bulk composition profiles, to get a first approximation to surface compositon for verification and interpretation of experimental results, and to predict general trends in materials performance.

Acknowledgement. This research was supported by the Korea Science & Engineering Foundation (Contract No. 893-0304-004-2).

References

1. M. P. Seah, *Surface Sci.*, **80**, 8 (1970).
2. D. E. Mencer, D. L. Cocke, and C. Yoon, *Surface Interface Anal.*, **17**, 31 (1991).
3. M. P. Seah, *J. Catal.*, **57**, 450 (1979).
4. K. Wandelt and C. R. Brundle, *Phys. Rev. Lett.*, **46**, 1529 (1981).
5. F. L. Williams and D. Nason, *Surface Sci.*, **45**, 377 (1974).
6. G. A. Somorjai, "Chemistry in Two Dimension", Cornell University Press, Ithaca, New York (1981).
7. A. R. Miedema, *Z. Metallkd.*, **69**, 455 (1978).
8. "CRC Handbook of Chemistry and Physics" (R. C. Weast and M. J. Astle, eds.), CRC Press, Boca Raton, Florida (1980).
9. R. Hultgren, P. A. Desai, D. T. Hawkins, M. Gleiser, and K. K. Kelly, "Selected Values of the Termodynamic Properties of Binary Alloys", American Society for Metals, Metals Park, Ohio (1973).
10. M. Guttmann, *Surface Sci.*, **53**, 213 (1975).
11. K. A. Gschneidner, Jr., in "Advances in Research and Applications, Vol. 16" (F. Seitz and D. Turnbull, eds.), Academic Press, New York (1964).
12. M. P. Seah, in "Practical Surface Analysis by Auger and X-ray Photoelectron Spectroscopy" (D. Briggs and M. P. Seah, eds.), John Wiley & Sons, Chichester (1983).
13. K.-J. Kim, D.-W. Moon, and K.-W. Lee, *J. Korean Vac. Soc.*, **1**, 106 (1992).
14. M. S. Hedge and T. S. S. Kumar, and R. M. Mallya, *Appl. Surface Sci.*, **17**, 97 (1983).

Stereoselective Reduction of 2-(1,3-dithian-2-yl)-pentan-3-one-with Baker's Yeast

Shin-Wook Kang, Won-Taek Oh†, and Jung-Han Kim*

Department of Food Engineering, Yonsei University, Seoul 120-140
†Korea Advanced Food Research Institute, Seoul 137-060

Received October 27, 1992

Asymmetric reduction of ketones with baker's yeast (*Saccharomyces cerevisiae*) is significantly being recognized as a useful method to obtain chiral building blocks for the synthesis of natural products[1]. β-Ketoesters are the extensibly studied as the substrates of baker's yeast reduction[2]. But the studies on the baker's yeast reduction of 2-methyl-3-oxopentanoate to the corresponding chiral hydroxyester have been limited until now[3].

Recently, our laboratory reported the baker's yeast reduction of alkyl 2-methyl-3-oxopentanoate to the corresponding *anti*-2-methyl-3-hydroxy-pentanoate with relatively low enantioselectivity (34-66% e.e.) in spite of high diastereoselectivity (93-99%)[4].

Therefore, to improve the enantioselectivity of the baker's yeast reduction, we replaced ester group of 2-methyl-3-oxopentanoate with 1, 3-dithian-2-yl group[5].

In this paper, we wish to report the highly diastereo-and enantioselective reduction of 2-(1,3-dithian-2-yl)-pentan-3-one **1** with baker's yeast to prepare 2-(1,3-dithian-2-yl)-pentan-3-ol **2a** as a novel chiral building block (Scheme 1).

The starting material **1** was prepared by thioacetalization of **3** with propanedithiol and $BF_3\cdot Et_2O$[6] followed by Swern oxidation of **4** with DMSO-TFAA[7] (Scheme 2)[8].

A typical procedure of the baker's yeast reduction is as